

## CARM DRIVER FOR HIGH FREQUENCY RF ACCELERATORS

B.G. Danly, J.S. Wurtele, K.D. Pendergast, and R.J. Temkin  
Plasma Fusion Center  
Massachusetts Institute of Technology  
Cambridge, MA 02139

### Abstract

The CARM is a promising source of microwave power for the next generation of linear collider. Designs for a high-power 17.136 GHz cyclotron autoresonance maser (CARM) amplifier, utilizing a 700 kV pulse-modulator and a 1.2 MeV linear induction accelerator, are presented.

### I. Introduction

The next generation of TeV  $e^+e^-$  linear colliders of reasonable length and cost will require<sup>1-3</sup> at least an order-of-magnitude increase in the accelerating gradient above the  $\sim 10 - 20$  MeV/m that can be presently achieved using conventional S-band klystron drivers. In order to obtain these increased accelerating gradients, the rf peak power and frequency must be increased substantially. The rf peak power breakdown limit is increased by increasing the frequency and decreasing the rf pulse length.

At present, designs for the next generation collider have settled on 17.136 GHz as a reasonable choice for the operating frequency.<sup>4,5</sup> The typical peak power that will be required per source is in the 500 MW to 1 GW range, with rf pulse lengths in the neighborhood of 25-50 ns.<sup>4,5</sup> For such a design, accelerating gradients may be on the order of 200 MeV/m.

Recently, there has been considerable theoretical interest in the cyclotron autoresonance maser (CARM).<sup>6-9</sup> The CARM is similar to a gyrotron, except that the electromagnetic wave propagates with a phase velocity close to the speed of light. The CARM typically employs relativistic electron beams with pitch angles ( $\alpha = v_{\perp}/v_{\parallel}$ ) smaller than that of the gyrotron. However, unlike gyrotrons and free-electron lasers, there are few experimental demonstrations of the CARM.<sup>10-12</sup> To date, work in the Soviet Union<sup>10,11</sup> has concentrated on CARM oscillators. Experimental work at MIT has demonstrated single-pass superradiant operation at 35 GHz, and, more recently, CARM amplifier operation at 35 GHz with  $\sim 25$  dB gain and saturated output powers of  $\sim 10$  MW. These results have been obtained in the CARM regime with a 1.5 MeV, 260 A beam from a Marx Accelerator.<sup>12</sup> A 140 GHz CARM amplifier utilizing a 450 kV electron beam generated from a SLAC 5045 klystron gun is also being assembled.<sup>13</sup>

The CARM amplifier has some potential advantages over the gyrokystron amplifier. Because the electromagnetic wave which propagates in the waveguide circuit is far from cut-off, large diameter waveguides may be used. In contrast, the guide size required for a gyrokystron amplifier circuit is smaller for a given frequency and mode because the wave is much closer to cut-off. For this reason, fundamental mode operation in large diameter waveguides is possible in the CARM at higher frequencies. On the down side, the CARM interaction is quite sensitive to velocity spread.

The CARM has the potential to operate as a high-gain, high-efficiency, high-power amplifier in the frequency regime applicable to the next generation colliders. In design of a high-peak power CARM amplifier, the electron beam energies which result in the most attractive operation are typically in the 0.5 - 2 MeV range. Consequently, beam generation for a high-power CARM

amplifier is well suited to two accelerator technologies. Both high-voltage (500 kV - 1 MV) SLAC-type pulse modulators and linear induction accelerators can be used for e-beam generation. For CARM designs based on induction accelerators, the peak beam powers and beam pulse durations result in the generation of rf pulses which are already well suited to the requirements of future colliders. An important alternative, however, is the use of conventional high-voltage pulse modulators to produce 0.5 - 1  $\mu$ s rf pulses, which are then compressed using binary energy compressors.<sup>14,15</sup> Such a combination may result in an attractive alternative to systems which utilize induction accelerators.

We have carried out a design study of both a pulse-modulator driven CARM amplifier operating with a 700 kV electron beam and an induction accelerator driven CARM amplifier with a 1.2 MeV electron beam. These designs are attractive for a proof-of-principle CARM amplifier experiment. Results of this design study are presented in this paper.

### II. Theory

The CARM interaction occurs when electrons undergoing cyclotron motion in an axial magnetic field ( $\mathbf{B} = B\hat{e}_z$ ) interact with an electromagnetic wave ( $\omega, \mathbf{k}$ ) with wavevector nearly parallel to the axial field  $\mathbf{B}$ . The resonance condition is then  $\omega - \mathbf{k} \cdot \mathbf{v} = s\Omega_c$ , where  $s$  is the harmonic number and  $\Omega_c$  is the relativistic cyclotron frequency defined by  $\Omega_c \equiv \Omega_{c0}/\gamma \equiv eB/\gamma mc$ . The well-known resonance condition for the CARM is thus  $\omega = s\Omega_{c0}/\gamma(1 - \beta_{\parallel}/\beta_{ph})$  where  $\gamma$  and  $\beta_{\parallel}$  are the electron energy and velocity in the  $\hat{z}$  direction. The wave phase velocity is given by  $\beta_{ph} \equiv v_{ph}/c = \omega/c k_{\parallel}$ . As is apparent from the resonance condition, the CARM is capable of operation at a large Doppler upshift from the cyclotron frequency (in contrast to the gyrotron). For  $\gamma_0^2 \gg 1, \beta_{\perp 0} \approx 1/\gamma_0$ , and  $\beta_{ph} \approx 1$ , there is a  $\gamma_0^2$  frequency upshift from the relativistic cyclotron frequency  $\Omega_c$  (or a  $\gamma_0$  upshift from the nonrelativistic cyclotron frequency,  $\Omega_{c0}$ ). For the numerical results given here, we consider only CARM operation at the fundamental of the cyclotron frequency ( $s = 1$ ).

The nonlinear equations for the CARM amplifier in a waveguide are derived by assuming that 1) the electromagnetic wave propagates in a fixed TE waveguide mode, 2) the particle motion is accurately described by considering only a single harmonic, and 3) drifts in the particle guiding centers are negligible. The MIT CARM amplifier code SPOT includes the following effects: harmonic interactions, arbitrary TE waveguide mode, annular or solid electron beams, waveguide losses, energy, momentum, and guiding center spreads (gaussian or uniform loading), pre-bunched electron beams, and a linearly tapered axial magnetic field. This code is described elsewhere.<sup>13</sup>

### III. Design of a 700 kV Pulse-Modulator-Driven 17 GHz CARM Amplifier

We have carried out designs for a long pulse (1  $\mu$ s) CARM amplifier experiment utilizing our 700 kV, 1  $\mu$ s pulse modulator and a 700 kV, 175 A electron gun. For operation with pulse

lengths of  $1 \mu\text{s}$ , the design of the CARM amplifier must optimize the device efficiency within the constraints imposed by the requirement that the amplifier not be susceptible to absolute instabilities. Because the  $1 \mu\text{s}$  pulse length is significantly longer than the typical e-folding times of the absolute instability, the design parameters of the device must be well within the calculated stability limits. We have carried out a preliminary design of a 17.136 GHz CARM amplifier using a 700 kV electron gun. The design parameters are presented in Table 1.

**Table 1**  
700 kV CARM Amplifier Design

Parameter	Design Value
Beam Energy	700 keV
Beam Current	175 A
$R_w$	1.3 cm
$\beta_{ph}$	1.0882
$\alpha$	0.709
$B_{z0}$	4.65 kG
$P_{in}$	10 kW
$P_{out}$	36.8 MW
$\eta_T$ , untapered	21.8 %
$z_{sat}$ , untapered	0.263 m
$\eta_T$ , $B_z$ taper	30.0 %
$z_{sat}$ , tapered	0.98 m
Detuning ( $\Delta_0$ )	0.0

For a fixed beam voltage and current of 700 kV and 175 A, the beam  $\alpha$  value ( $\alpha \equiv p_{\perp}/p_{\parallel}$ ) corresponding to the threshold for absolute instability is given by  $\alpha = \alpha_c$ , with  $\alpha_c$ . The critical pitch may be calculated by a Bers-Briggs pinch-point analysis of the CARM dispersion relation.<sup>16</sup> In these calculations, no wall loss has been assumed. The critical pitch will be a function of the magnetic field, which will in turn be a function of the waveguide radius  $R_w$  and the frequency  $\nu$  for a given detuning from resonance. The efficiency for a  $TE_{11}$  mode CARM amplifier operating at 17.136 GHz is plotted as a function of waveguide radius in Fig. 1. The axial magnetic field is uniform for these simulations. Also shown is the critical pitch ( $\alpha_c$ ) at each waveguide radius assuming resonant magnetic field. The

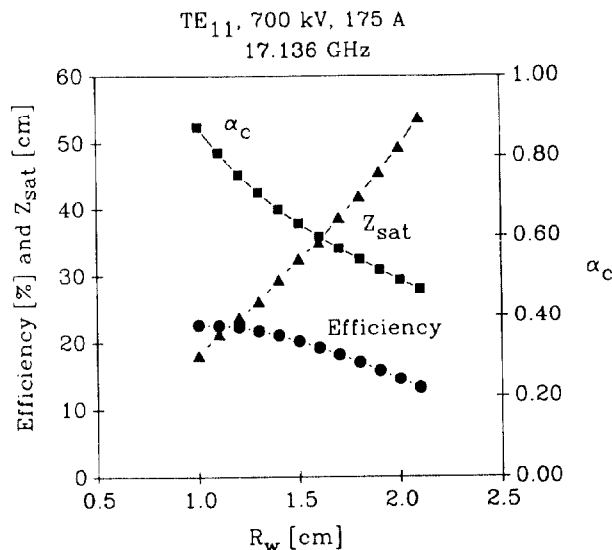


**Fig. 1** Efficiency, saturation length, and critical  $\alpha$  versus waveguide radius for 700 kV,  $TE_{11}$  mode 17.136 GHz CARM amplifier with no magnetic field taper.

value of  $\alpha$  used for each waveguide radius is  $\alpha = \alpha_c(R_w)$ . The critical pitch is high at small guide sizes because the magnetic field required for resonance is closer to the grazing magnetic field. The optimum efficiency for this untapered magnetic field case is approximately 22%. Consequently, a magnetic field taper will be required to enhance the efficiency of this 700 kV,  $TE_{11}$  mode design. A preliminary design of a 700 kV experiment including a linear magnetic field taper has yielded a design with 30% efficiency. Further efficiency enhancement should be possible with optimized magnetic field taper profiles and with other techniques such as waveguide radius tapering and prebunching.

#### IV. Design of a 1.2 MeV Induction-Linac-Driven 17 GHz CARM Amplifier

We have also carried out design studies of a CARM amplifier utilizing a 1.2 MeV linear induction accelerator (LIA). For the short pulse lengths obtained with induction accelerators, CARM operation in the higher order modes may be feasible. For operation in higher order modes, such as the  $TE_{13}$ , the beam may be stable in the  $TE_{13}$  mode (at the lower intersection) but the beam may be unstable in lower order modes. For long pulse operation these lower order modes are potentially serious,<sup>16-18</sup> as there is ample time for the absolute instability to reach saturation. However, for the short e-beam pulse lengths typically obtained from induction linacs, amplification on the desired convective instability may be possible for time scales which are short compared to the time required for the unstable modes to grow significantly. Such behavior has been recently seen in particle-in-cell code simulations.<sup>18</sup>

From the standpoint of device efficiency, operation in higher order modes is desirable for cases where the beam current is high. If the operating mode is fixed, the CARM efficiency in a uniform axial magnetic field has an optimum at a specific value of the current.<sup>6,8</sup> For the designs considered here, the desired operating currents are well above this optimum current if the operating mode is  $TE_{11}$ . Operation in higher order modes increases the current at which the optimum efficiency occurs.

The preliminary design parameters of a  $TE_{13}$  mode 17.136 GHz CARM amplifier are presented in Table 2. The untapered efficiency is 33%, and the efficiency obtained with a linear ax-

**Table 2**  
LIA-Driven  $TE_{13}$  Mode CARM Amplifier Design

Parameter	Design Value
Beam Energy	1.2 MeV
Beam Current	500 A
Pulse Length	50 ns
$\alpha$	0.6
Frequency	17.136 GHz
Mode	$TE_{13}$
Guide Radius	5 cm
$\beta_{ph}$	1.137
$P_{in}$	10 kW
$\eta$ , untapered	33.6%
$\eta$ , -0.5%/cm taper	46.4%
$z_{taper}$	0.45 m
$z_{sat}$	0.96 m
$P_{sat}$	278 MW
$B_0$	4.94 kG
Detuning ( $\Delta_0$ )	0.4

ial magnetic field taper is 46%. The results are obtained with the MIT CARM code SPOT. Higher efficiencies should be possible with better optimized (non-linear) tapers, as well as with tapering of the waveguide radius. Negative tapers can produce significant increases in the efficiency; Fig. 2 is a plot of the efficiency as a function of the linear taper rate for four different axial positions at which the taper begins. The taper rates required for significant efficiency enhancement are modest.

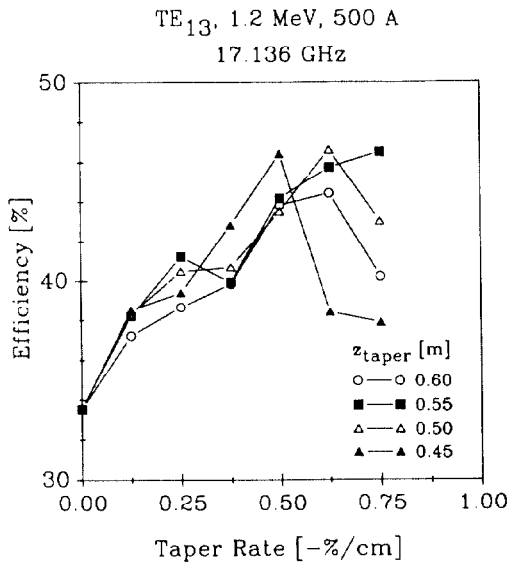


Fig. 2 LIA-Driven CARM Amplifier Efficiency versus Magnetic Field Taper Rate. The untapered saturation length is 0.6 m;  $z_{taper}$  is the starting position of the axial taper.

The stability of this TE<sub>13</sub> design with regard to the TE<sub>11</sub> and TE<sub>12</sub> modes can be estimated by a comparison of the absolute instability temporal growth rates for the TE<sub>11</sub> and TE<sub>12</sub> modes with the e-beam pulse length. The actual temporal growth rate for the absolute instability should be significantly reduced by the presence of drive power at the frequency corresponding to the convective instability. Furthermore, the addition of waveguide wall loss for the lower frequencies will also help prevent instability.

## V. Conclusions

The CARM amplifier is a promising source of high frequency radiation for future linear colliders. Initial design studies indicate that attractive CARM designs exist which utilize either pulse-modulator technology or induction linac technology for generation of the electron beam. Interaction efficiencies are in the 30 – 50% range; higher efficiencies should be possible with nonlinear tapers.

## Acknowledgements

This research is supported by the Department of Energy. We are grateful to the SLAC Klystron Division for providing the 5045 klystron gun used in our 140 GHz CARM experiments.

## References

- <sup>1</sup>P. Wilson, IEEE Trans. Nucl. Sci. **NS-28**, 2742 (1981).
- <sup>2</sup>P. Wilson, Technical Report SLAC PUB 3227, SLAC (1983).
- <sup>3</sup>A. Sessler, Physics Today **41**, 26 (1988).
- <sup>4</sup>R. Palmer, Technical Report SLAC-PUB-4295, Stanford Linear Accelerator Center (1987).
- <sup>5</sup>T.G. Lee, private communication, June, 1988.
- <sup>6</sup>V. Bratman, N. Ginzburg, G. Nusinovich, M. Petelin, and P. Strelkov, Int. J. Electron. **51**, 541 (1981).
- <sup>7</sup>A. Lin, Int. J. Electron. **57**, 1097 (1984).
- <sup>8</sup>A. Fliflet, Int. J. Electron. **61**, 1049 (1986).
- <sup>9</sup>K. Pendergast, B. Danly, R. Temkin, and J. Wurtele, IEEE Trans. Plasma Sci. **PS-16**, 122 (1988).
- <sup>10</sup>I. Botvinnik, V. Bratman, A. Volkov, N. Ginzburg, G. Denisov, B. Kol'chugin, M. Ofitserov, and M. Petelin, Pis'ms Zh. Eksp. Teor. **35**, 418 (1982).
- <sup>11</sup>I. Botvinnik, V. Bratman, A. Volkov, G. Denisov, B. Kol'chugin, and M. Ofitserov, Pis'ms Zh. Eksp. Teor. **8**, 1376 (1982).
- <sup>12</sup>G. Bekefi, A. DiRienzo, C. Leibovitch, and B. Danly, Appl. Phys. Lett. (1989) [To Be Published].
- <sup>13</sup>B. Danly, K. Pendergast, R. Temkin, and J. Davies, in *Proc. SPIE, Vol. 873* (1988).
- <sup>14</sup>Z. Farkas, Technical Report SLAC PUB 3694, SLAC (1985).
- <sup>15</sup>Z. Farkas and J. Weaver, Technical Report SLAC/AP-59, SLAC (1987).
- <sup>16</sup>J. Davies, Phys. Fluids **B1**, 663 (1989).
- <sup>17</sup>B. Danly, K. Pendergast, R. Temkin, and J. Wurtele, Proc. S.P.I.E. **1061** (1989) [To Be Published].
- <sup>18</sup>A. Lin, C. Lin, and K. Chu, IEEE Trans. Electron Dev. (1989) [To Be Published].